

Accepted on (14-03-2017)

## The Effect of $Al^{3+}$ Ions Concentration on DC Conductivity and Curie Temperature of Ni - Spinel Ferrite

Hussein A. Dawoud<sup>1,\*</sup>

<sup>1</sup>Department of Physics, Faculty of Science, Islamic University of Gaza, Gaza Strip, Palestine

\* Corresponding author

e-mail address: [hdawoud@iugaza.edu.ps](mailto:hdawoud@iugaza.edu.ps)

### Abstract

A series of Al substituted Ni spinel ferrites with the empirical formula  $NiAl_xFe_{2-x}O_4$ , where  $x = 0.0, 0.1, 0.2, 0.3, 0.4$  and  $0.5$ , were prepared by conventional ceramic double sintering method. DC electric properties and initial permeability ( $\mu_i$ ) were carried out for the prepared series of samples from room temperature to well beyond the Curie point temperature ( $T_C$ ). The thermal behavior of the DC electric conductivity for the prepared samples indicated that they act as semiconducting materials. On the other hand, DC electric conductivity is greatly affected when the  $Al^{3+}$  ions are increased. The DC electrical conductivity results were interpreted in terms of electron hopping model. The calculated activation energy in the ferrimagnetic region was less than that in paramagnetic region. The initial permeability showed constant values from room temperature to  $T_C$ , then it decreased sharply. The Curie temperature was determined from DC electrical properties and initial permeability.  $T_C$  was found to decrease with increasing of  $Al^{3+}$  ions.

### Keywords:

Spinel Ferrite,  
DC Electric,  
Curie Temperature,  
Inductance,  
Activation Energy.

### 1. Introduction:

Day by day, the demand for ferrites increases to meet the requirements of technological and industrial advances in various areas. Among them, spinel ferrites have received immense attention due to their novel magnetic, electric, optical, catalytic and dielectric properties (Suryanarayana et al 2014; Bato0 et al 2012; Singh et al 2012), memory storage capacity, mechanical hardness, chemical and thermal stability, easy to synthesize and reasonable cost (Mahmud et al 2016; Shahjahan et al 2014). Spinel ferrites have a wide extended applications encompass an impressive in different fields due to their interesting electric properties (Vagolu et al 2014). The properties of spinel ferrites depend upon several factors chemical compositions, preparation routes, distribution of

dopants and substitution into the lattice, sintering temperature and grain size (Suryanarayana et al 2014; Kumar et al 2014). The electrical properties of spinel ferrites are sensitive to their composition and microstructure, which in turn are sensitive to their processing conditions. Spinel ferrites have a general formula  $DFe_2O_4$  (D is divalent metal ions) (Shaata et al 2013; Shaata et al 2014]. The electrical properties of ferrites are mainly affected by cation distribution, non-magnetic and magnetic substitutions, amount of ferrous ( $Fe^{2+}$ ) present, sintering conditions, grain size and grain growth effects. The electrical conductivity ( $\sigma$ ) of spinel ferrites is prime importance as it gives valuable information about the conduction mechanism. The spinel ferrites are widely used in several electronic

devices due to noticeable electrical resistivity (from  $10^{-3}$  to  $10^{11}$  ohm-cm) (Suryanarayana et al 2014), low eddy current and reasonable cost (Mahmud et al 2016; Shaat et al 2014)]. The high and low resistivities of ferrites are mainly demonstrated according to cations distribution in tetrahedral ( $T_d$ ) and octahedral ( $O_h$ ) sites of the spinel structure and hopping mechanism. The high value of  $\sigma$  in ferrites is due to simultaneous existence of  $Fe^{2+}$  and ferric ( $Fe^{3+}$ ) into  $T_d$  and  $O_h$  sites. The low resistivity in ferrites links to the occupation of  $O_h$  sites by different D and  $Fe^{3+}$  ions. Both  $Fe^{2+}$  and  $Fe^{3+}$  ions are at  $O_h$  sites and conduction takes place when electrons move from  $Fe^{2+}$  to  $Fe^{3+}$  ions. The electrical mechanism and the change of conductivity ( $\sigma$ ) and the activation energy ( $E_a$ ) at Curie temperature ( $T_C$ ) and the relation of activation energies with composition can be modeled as semiconductors, electrons hopping, small polaron and phonon induced tunneling. Small polaron formation can find in materials whose conduction electrons belong to incomplete inner (d or f) shells, which due to small electron overlap; imply to form extremely narrow bands. These polarons have low activation energy in magnetic region, while more activation energy in non-magnetic regions. In the present study, we report the conductivity mechanism and Curie temperature of  $NiAl_xFe_{2-x}O_4$ .

## 2. Experimental:

### 2.1 Synthesize of the Samples:

The mixed polycrystalline ferrites  $NiAl_xFe_{2-x}O_4$ , where  $x$  is the percentage increment of Al<sup>3+</sup> ions on the compound which have the value  $0.0 \leq x \leq 0.5$ , were prepared by using the standard double sintering SSR by mixing pure metal oxides  $NiO$ ,  $Al_2O_3$ , and  $Fe_2O_3$ , 25.0 grams from high purity metal oxides were used to prepare each composition of the investigated polycrystalline spinel ferrites. The metal oxides were weighted using a sensitive electric balance (ADAM model PW124) with an accuracy  $1 \times 10^{-4}$  gm. The weighted metal oxides were mixed and then grounded to a very fine powder for 5 hr's. The mixed powder of metal oxides was pre-sintered at  $750^\circ C$  for 3 hr's soaking time using a laboratory Furnace (BIFATHERM model AC62). Then the prefired powder was well ground for 3 hours and pressed with hydraulic press under constant pressure of  $3 \times 10^8$  pa, by using a small quantity of butyl alcohol as a binding material. Some

samples were pressed in a disc shape with a diameter 11 mm and thickness (4-6) mm to measure resistance for all samples. Other samples were pressed in toroidal shape with an external diameter  $D_o$  of 9.3 mm, and internal diameter  $D_i$  of 4.7 mm with thickness (4-5) mm, for measuring inductance. After that, all samples were sintered at  $1200^\circ C$  for 5 hr's soaking time. After sintering process, the samples were cooled down gradually to room temperature. After that, the samples were polished to obtain uniform parallel surfaces.

### 2.2 Properties Measurements:

A digital multimeter temperature indicator (model 2010DMM) with resolution  $1^\circ C$  was connected with the thermocouple K(NiCr-NiAl) was used to measure temperature from room temperature up to 900 K.

A digital multimeter (model FLUKE -177) was used to measure the resistance of the samples from room temperature up to 800 K with step of three-degrees. The increasing of temperature was carried out gradually. The specific DC electric conductivity  $\sigma_{DC}$  ( $\Omega m$ )<sup>-1</sup> of the samples was calculated from the formula:

$$\sigma_{DC} = R^{-1} \frac{l}{A} \quad (1)$$

where,  $R$  is a resistance of the sample,  $l$  it's thickness which was measured by a micrometer of accuracy 0.01 mm,  $A$  is the cross-sectional area of the sample.

14 turns of an insulated wire were wrapped around the toroidal samples to measure the inductance as a function of temperature. The inductance as a function of initial permeability was measured directly using LCR meter model (GW- instek LCR-821), with series circuit and applied voltage of 1V and constant frequency of 20 KHz with accuracy of (0.05%).

## 3. Results and Discussion:

### 3.1 Temperature-Dependent of DC Electric Conductivity:

DC electrical conductivity ( $\sigma_{DC}$ ) is one of the useful characterization techniques to understand conductivity mechanism (lee et al 2006). The thermal dependence of  $\sigma_{DC}$  for the mixed Al-Ni spinel ferrites with different Al concentrations was investigated from room temperature to fit beyond the transition temperature i.e.  $T_C$ . The variation of  $\ln \sigma_{DC}$  versus the reciprocal of temperature ( $10^3/T$ ) is depicted in Figure 1. This Figure illustrates that,  $\ln \sigma_{DC}$  increases continuously

with the increasing of temperature. This confirms that the ferrite under investigation have the same behavior of various ferrite systems (Krishna et al 2012). The conduction mechanism of ferrites, also, depends on temperature. It is reported that, the electric conduction at lower temperature (below  $T_C$ ) is due to hopping electron between  $Fe^{2+}$  and  $Fe^{3+}$  ions, whereas at a higher temperature (above  $T_C$ ) is due to the hopping of polarons (Kumar et al 2001). In the hopping process the additional electron of  $Fe^{2+}$  ion requires little energy to move to an adjacent  $Fe^{3+}$  on  $O_h$  sites. The change in the  $Fe^{2+}$  ion content in the spinel ferrite lattice and/or the distance between them is crucial to the intrinsic resistivity of Ni-Al ferrite grains, including the intrinsic grain boundaries. If the introduction of another cation into the lattice causes a change in the valency distribution on the  $O_h$  sites, then the number of electrons potentially available for transfer will be altered. More charge carriers appear to be injected into the conduction process with increasing temperature as a result the  $\sigma_{DC}$  increases with increasing temperature. The  $\sigma_{DC}$  is seen to increase much more rapidly with increasing temperature as the samples undergo a ferrimagnetic to paramagnetic transition. This behavior may be attributed to the increase in drift mobility of the charge carriers.

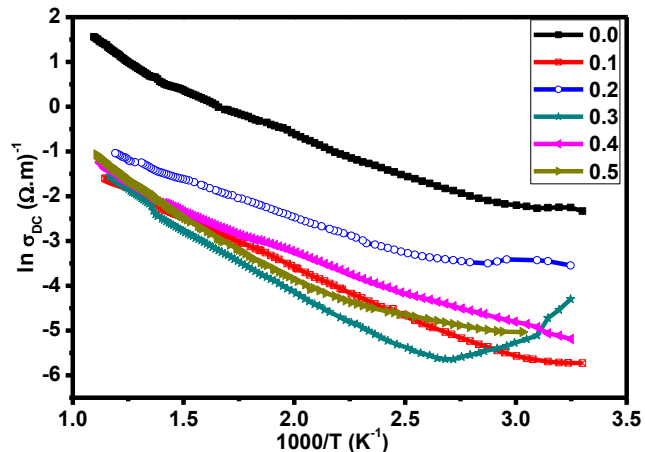


Figure 1 Variation of  $\ln \sigma_{DC}$  with  $(10^3/T)$  for the samples with different  $x$

Figure 2 follows Arrhenius (Krishna et al 2012), which presents  $\ln \sigma T$  versus  $(10^3/T)$ , in which the values of  $\ln \sigma T$  increased linearly with increasing of temperature up to  $T_C$  at which a slope changed. Similar behavior was reported by several researchers for different ferrite systems (Pal et al 1996). It was proved theoretically that at the  $T_C$  a change must occur in the gradient of the

straight line and the magnitude of the change depends on the exchange interaction between the outer and the inner electrons which alter the  $T_C$ . Generally, the change of slope is attributed to change in conductivity mechanism. The dependence of the DC electric conductivity on temperature, which is demonstrated in the Figure 2 fulfills the Arrhenius relation

$$\sigma = \frac{S}{T} e^{(-E_a/kT)} \quad (2)$$

where  $S$  is a constant given by  $(ne^2 d^2 \nu / k)$ ,  $n$  is the number of the charge carriers,  $e$  is the electron charge,  $d$  is the distance between the nearest neighbor cations,  $\nu$  is the frequency of the vibration of the crystal lattice,  $k$  is the Boltzmann constant and  $E_a$  is the activation energy.

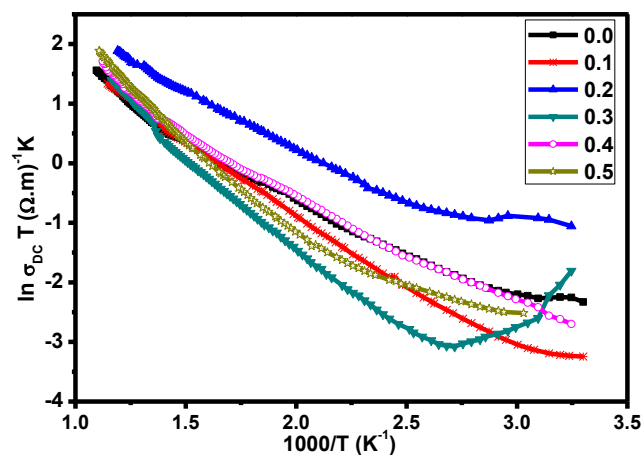


Figure 2 Variation of  $\ln \sigma T$  with  $(10^3/T)$  for the samples with different  $x$

### 3.2 Composition Dependence of DC Electrical Conductivity

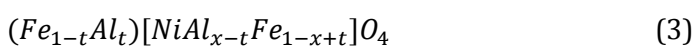
The activation energies in both regions ferrimagnetic ( $E_f$ ) and paramagnetic ( $E_p$ ) for the studied compositions were calculated using the two slopes in Figure 2 and equation (2). The calculated values of activation energies  $E_f$  and  $E_p$  for the given ferrite system were tabulated in Table (1). It is noticed that, the values of  $E_p$  are greater than of the values of  $E_f$ . (Kadam et al 2010) reported that, if substituted ions occupy  $T_d$  sites without disturbing  $O_h$  site, then  $E_a$  almost remains unaltered, whereas if substituted ions occupy  $O_h$  sites then the effect on  $E_a$  is greater. It is,

also, reported that hopping between ions of same metals on  $O_h$  site needs lower value of  $E_a$  than for ions of different metal (awoud et al 2016). As indicating in Table 1 the values of activation energy can be divided into groups lower than 0.2 eV and greater than 0.2 eV. For the values of activation energy lower than 0.2 eV the conduction mechanism is predominantly due to the electron hopping between  $Fe^{2+}$  and  $Fe^{3+}$  (Sattar 2003). Moreover, for the values of activation energy greater than 0.2 eV the conduction mechanism is due to the small polaron.

**Table 1** Values of the ferrimagnetic activation energy  $E_f$  and paramagnetic activation energy  $E_p$

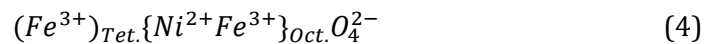
x	Activation Energy	
	$E_f$ (eV)	$E_p$ (eV)
0.0	0.17	0.31
0.1	0.19	0.22
0.2	0.16	0.21
0.3	0.25	0.39
0.4	0.16	0.31
0.5	0.25	0.35

The electric conductivity in the ferrites associates with the presence of the ions for the same element in more than one valence state, these ions are distributed over the crystallographically inequivalent sites, herein  $T_d$  and  $O_h$  (Shaht 2012; Dawoud et al 2006). In line with, the cations distribution is important to explain the electric conduction mechanism. Herein, the cations distribution of Ni-Al ferrite is expected to be



where  $0 \leq t \leq 0.1$ . According to the given cations distribution in (3), the change of the electric conductivity with increasing of the  $Al^{3+}$  ions is explained for the mixed Ni-Al spinel ferrite. It is obviously from formula (3) that, with increasing of the  $Al^{3+}$  ions in  $O_h$  sites and slightly in  $T_d$  sites, this implies predominantly to decrease the  $Fe^{3+}$  ions in the  $O_h$  sites. This may be disturb the bond  $Fe^{2+} - O^{2-}$  of  $T_d$  and  $O_h$  sites in the spinel lattice [13]. The  $Fe^{2+} - O^{2-}$  bond exerted by the  $Fe^{2+}$  ions that is formed in the samples during the sintering process. Noting that, the sintering process effects on the number of the  $Fe^{2+}$  ions in each site.

For the sample with  $x = 0.0$ , which is completely inverse spinel structure, the cations distribution in (4) becomes



It is clearly; that the two cations, i.e.  $Ni^{2+}$  and  $Fe^{3+}$ , occupied the  $O_h$  sites is responsible for electrical conduction in nickel ferrite, which can be described as the following [17]



It has been assumed that the electrons, which participate in the formula (5) exchange process, are strongly coupled to the lattice and tunnel from one site to other due to a phonon-induced transfer mechanism. From formula (5) and (6), there is a possibility to combine of ( $e^-$  and  $h^+$ ) in the  $O_h$  sites. This implies to reduce the number of electrons in the  $O_h$  sites, which leads to decrease the electric conductivity. On the other hand, the electronic distribution of the  $Fe^{2+} - O^{2-}$  bond is greatly affected when the  $Al^{3+}$  ions are increased as shown in Figure 1.

### 3.3 The Initial Permeability:

The initial permeability ( $\mu_i$ ) of the ferrimagnetic materials which results from the domains walls motion and spin rotational (Shaht 2012). It depends upon the magnetization, the ionic structure and the degree of domain walls continuity across the grain boundary layers (Dawoud et al 2006). It is found that  $\mu_i$  varies with different conditions such as the soaking time, the sintering temperature, the time of sintering, the porosity, the defects introduced and atmosphere of firing due to the sintering process (Shaht 2012).

The relation between the inductance (L) of a closed packed coil (toroid) knitted around a substance and its permeability is given by (Jebeli et al 2013)

$$\mu = \frac{2\pi L}{N^2 l \ln\left(\frac{R_o}{R_i}\right)} \quad (7)$$

where  $N$  is the number of turns,  $R_o$  and  $R_i$  are outer and inner radii of toroid, respectively, and  $l$  is thickness of toroid. The permeability of the substance can be expressed by

$$\mu = \mu_o \mu_r \quad (8)$$

with  $\mu_0$  is the free space permeability and  $\mu_r$  is the relative permeability. However,  $\mu_r$  at low excitation level and constitutes the most important means for the comparison of soft magnetic materials can be defined as the initial permeability ( $\mu_i$ ). Therefore, an expression for the initial permeability can be derived as follows

$$\mu_i = \frac{2\pi L}{\mu_0 N^2 l \ln\left(\frac{R_o}{R_i}\right)} \quad (9)$$

The magnetization ( $M$ ) of a specific core material located inside the coil has the following expression (Nabiyouni et al 2010)

$$M = \chi_m H = \frac{(\mu_i - 1)}{4\pi} H \quad (10)$$

where,  $\chi_m$  is the magnetic susceptibility,  $H$  is the magnetic field produced by the coil. By using equations (9) and (10), it can be found that

$$M = \left[ \frac{L}{2\mu_0 N^2 l \ln\left(\frac{R_o}{R_i}\right)} - \frac{1}{4\pi} \right] H \quad (11)$$

It is clear from equation (11) that,  $M$  is proportional to  $L$ . This means that, if  $M$  changes with temperature  $\mu_i$  also changes. Therefore, the transition or Curie temperature can be indicated from the variation of  $\mu_i$  with temperature. The thermal spectra of  $\mu_i - T$  curve can be taken as a test function of homogeneity of the ionic structure of the sample (Dawoud et al 2006). It depends strongly on the preparation conditions, since, these ferrites are in polycrystalline form (Shaht 2012). Inductive sensing is based on measuring the variation of  $\mu_i$  for the toroid shape specimens for all prepared samples of mixed Ni-Al ferrites. Figures 3 and 4 depict the variation of  $\mu_i$  versus temperature from room temperature to fit beyond  $T_C$ . It is noticed that,  $\mu_i$  is mostly constant up to transition happens at which drop of  $\mu_i$  is occurred for all sample as in Figures 3 and 4. This means that the samples under investigation have transition from ferrimagnetic at lower temperature "below  $T_C$ " to paramagnetic at higher temperature "above

$T_C$ ". It is found that the transition temperatures increased as the Al content increased.

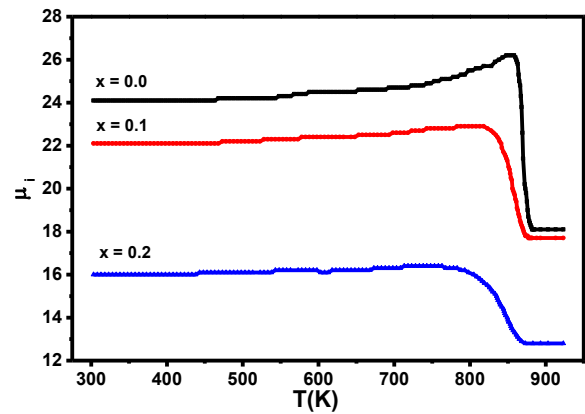


Figure 3 Variation of  $\mu_i$  with temperature for the samples with  $x = 0.0, 0.1$  and  $0.2$

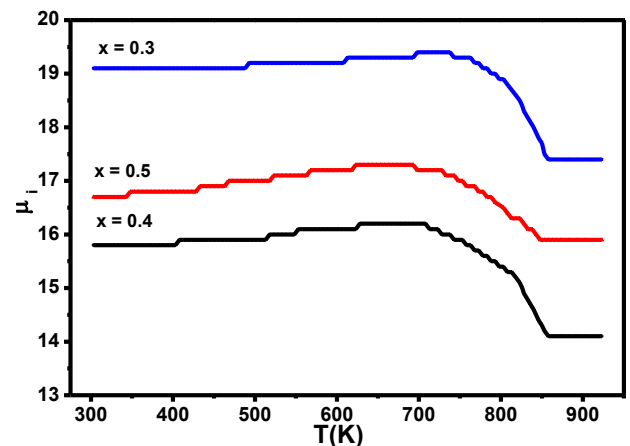


Figure 4 Variation of  $\mu_i$  with temperature for the samples with  $x=0.3, 0.4$  and  $0.5$

### 3.4 Composition Dependence of Curie Temperature:

The values of  $T_C$  for the mixed Ni-Al spinel ferrite are determined from the DC electric conductivity and the initial permeability measurements which are listed in Table 2. As shown in this table, there is a small deviation of the  $T_C$  values from the induction and the conductivity measurements. This indicates that, the magnetic transition can be manifested in the transport property. The variation of  $T_C$  with composition  $x$  is plotted in Figure 5. From this figure it is noticed that  $T_C$  is increased as  $x$  increases i.e. increasing of Al<sup>3+</sup> ions. As it was represented in Figure 5, the  $T_C$  decreased



continuously with increasing of the Al<sup>3+</sup> ions. The same behavior was, also, observed by other workers (Joshi et al 1986). This is attributed to the addition of the non-magnetic Al<sup>3+</sup> ions that replaced the magnetic Fe<sup>3+</sup> ions at the O<sub>h</sub> sites, thus; the number of the Fe<sup>3+</sup> ions decrease at the O<sub>h</sub> sites. This tends to decrease the strength of T<sub>d</sub> and O<sub>h</sub> exchange interactions of the type Fe<sub>T</sub><sup>3+</sup> - O<sup>2-</sup> - Fe<sub>O</sub><sup>3+</sup>, apart from decreasing number of bonds or linkages between the magnetic ions (Gillfo 1958).

**Table 2** Values of T<sub>C</sub> which determined by induction and DC conductivity measurements for the mixed Ni -Al spinel ferrite

x	Initial Permeability Results	DC conductivity Results
	T <sub>C</sub> (K)	T <sub>C</sub> (K) ± 10%
0.0	860	845
0.1	823	772
0.2	805	758
0.3	788	738
0.4	768	727
0.5	733	693

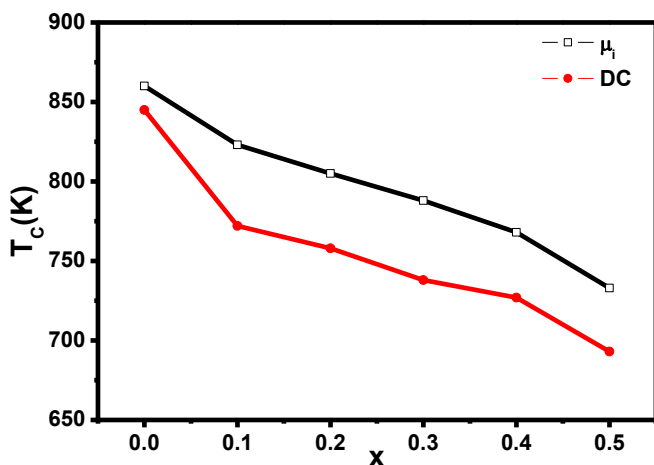


**Figure 5** Variation of T<sub>C</sub> with Al ratio "x"

#### 4. Conclusions:

Substitution of the non-magnetic Al<sup>3+</sup> ions in Ni spinel ferrite has a tremendous influence on the electric properties. From this study, we concluded that:

- DC conductivity exhibits an excellent behavior of semiconductor materials.
- The activation energy in paramagnetic region is greater than ferrimagnetic region. This attributed to the existence of small polaron-hopping.
- The initial permeability can be used to determine the Curie point temperature, which showed decreasing with increasing of Al<sup>3+</sup> ions.
- It is found that transition occurs for all samples Furthermore, Al content has significant influence on the electric properties, for Ni ferrites; so, the mixed Ni-Al spinel ferrite is considered a soft ferrite material, which is proved an interest material for technological and scientific and industrial applications

#### References:

- Batoo K. M. and Ansari M. S., (2012), Low temperature-fired Ni-Cu-Zn ferrite nanoparticles through auto-combustion method for multilayer chip inductor applications *Nanoscale Research Letters*, , 7(112), 2-14.
- Dawoud H., A-Ouda L. and Shaat S. K. K., (2016) Investigation of the Effect of Zn Ions Concentration on DC Conductivity and Curie Temperature of Ni-spinel Ferrite, *American Journal of Materials Science and Application*, 4(2), 11-17
- Dawoud H. A. and Shaat S.K.K., (2006) Initial Permeability and DC Conductivity of Cu - Zn Ferrite *The Islamic university Journal*, 114, 165-182.
- Gillfo M. A.. (1958) Superexchange Interaction Energy for Fe<sup>3+</sup>-O<sup>2-</sup>-Fe<sup>3+</sup> Linkages, *Phys. Rev*, 109, 777-781.
- Jebeli M S and Mohamed N M B, (2013) Synthesis and Charactrization of Ni-Zn Ferrite Based Nanoparticles by Sol-Gel Technique *IJMSI*, , 1(1), 45-53.
- Joshi H. H. and Kulkarni R. G., (1986) Susceptibility, magnetization and Mössbauer studies of the Mg-Zn ferrite system *J. of Mat. Sci.*, , 21, 2138-2142
- Kumar K. V., Sridhar R., Ravinder D. and Krishna K. R., (2014) Structural Properties and Electrical Conductivity of Copper Substituted Nickel Nano

- Ferrites *International Journal of Applied Physics and Mathematics*, 4(2), 113-117.
- Krishna K. R., Kumar K. V. and Ravinder D., (2012), Structural and Electrical Conductivity Studies in Nickel-Zinc Ferrite, *Advances in Materials Physics and Chemistry*, 2(3), 185-191
- Kumar K.V. and Ravinder D., (2001) Electrical Transport Properties of Erbium Substituted Ni-Zn Ferrites, *Int. J. Inorg. Mater.*, 3(7), 661-666.
- Krishna K. R., Kumar K.V. and Ravinder D., (2012) Structural and Electrical Conductivity Studies in Nickel-Zinc Ferrite, *Adv. Mater. Phys. Chem.*, 2, 185-191.
- Kadam G.B., Shelke S.B. and Jadhav K. M., (2010) Effect of Zinc on A. C. Susceptibility and D. C. Resistivity of Ni<sub>1-x</sub>Zn<sub>x</sub>Fe<sub>2-y</sub>Eu<sub>y</sub>O<sub>4</sub> *Journal of Electronic and Electrical Engineering*, 1(1), 03-11.
- Lee S. W. and Kin C. S., (2006) Superparamagnetic Properties Ni-Zn Ferrite for Nano-Bio Fusion Applications *J. of magnetism and magnetic material*, 304(1), 418-420.
- Mahmud A., Islam S. and Nahar S. S., (2016) Effect of SN (Tin) Alloying on Ni-Zn Ferrites Characteristics *IJAMSE*, 5(1), 1-10.
- Nabiyouni G., Fesharaki M. J., Mozafari M. and Amighian J., (2010) Characterization and Magnetic Properties of Nickel Ferrite Nanoparticles Prepared by Ball Milling Technique *J. Chem. Phys. Lett.*, 27(12), 126401-126404.
- Pal M, Brahma P, chakravorthy D., (1996) Magnetic and electrical properties of nickel-zinc ferrites doped with bismuth oxide *J Magn Mater*, 152(3), 370-374.
- Sattar A.A., (2003) Temperature Dependence of the Electrical Resistivity and Thermoelectric Power of Rare Earth Substituted Cu - Cd ferrite *Egypt. J. Sol.*, 26(2), 133-120.
- Shahjahan Md., Ahmed N. A., Rahman S. N., Islam S. and Khatun N., (2014) Structural and Electrical Characterization of Ni-Zn Ferrites *IJETCAS*, 13(104), 20-25.
- Shaht S. K. K., (2012) Advanced Ferrite Technology, *LAMBART Academic Publishing*.
- Shaht S. K. K., Swart H. C. and Ntwaebborwa O. M., SA Institute of Physics, (2013) White cathodoluminescence from Zn<sub>0.3</sub>Mg<sub>0.7</sub>Al<sub>2</sub>O<sub>4</sub>:Tb<sup>3+</sup>,Eu<sup>3+</sup> ISBN: 978-0-620-62819-8.
- Shaht S. K.K., Swart H. C. and Ntwaebborwa O. M., (2014) Tunable and white photoluminescence from Tb<sup>3+</sup>-Eu<sup>3+</sup> activated Ca<sub>0.3</sub>Sr<sub>0.7</sub>Al<sub>2</sub>O<sub>4</sub> phosphors and analysis of chemical states by X-ray photoelectron spectroscopy *Journal of Alloys and Compounds*, 587, 600-605.
- Shaht S. K. K., Swart H. C. and Ntwaebborwa O. M., (2014) Investigation of luminescent properties of Ca<sub>0.3</sub>Sr<sub>0.7</sub>Al<sub>2</sub>O<sub>4</sub>:Tb<sup>3+</sup>,Eu<sup>3+</sup> excited using different excitation sources *Journal of Electron Spectroscopy and Related Phenomena*, 197, 72-79.
- Singh S., Singh M., Ralhan N. K., Kotnala R. K. and Verma K. C., (2012) Improvement in ferromagnetism of NiFe<sub>2</sub>O<sub>4</sub> nanoparticles with Zn doping *Adv. Mat. Lett.*, 3(6), 504-506.
- Suryanarayana B., Mouli K. C., Raghavendra V. and Parvateesam B. B., (2014) Synthesis and Magnetic studies of Ni-Cu-Zn ferrite Nanocrystals *IJRFB*, 1, 92-94.
- Vagolu V. K., Samatha K., Mouli K. C., Kiran J. N. and Sanasi P. D., (2014) Preparation and Characterization of Polycrystalline Mixed Nickel Zinc Ferrites for Dielectric Properties and Practical Application *Int J Pharm Bio Sci*. 5 (3), 159 - 175.

#### تأثير تركيز أيونات الألومنيوم على التوصيل في حالة التيار المستمر وعلى درجة حرارة كوري للنيكل اسبنل فيرايت

**كلمات مفتاحية:**  
إسبنل فيرايت،  
التيار المستمر،  
درجة حرارة كوري،  
المحثة،  
طاقة التنشيط.

لقد استخدمت الطريقة السيراميكية التقليدية في تحضير مجموعة من عينات الألومنيوم نيكل فريت  $NiAl_xFe_{2-x}O_4$  حيث أن  $x = 1.0, 0.2, 0.3, 0.4, 0.5$  لقد تم قياس النفاذية المغناطيسية ( $\mu_i$ ) والتوصيلية الكهربائية في حالة التيار المستمر ( $\sigma_{DC}$ ) للعينات المذكورة من درجة حرارة الغرفة حتى درجة حرارة كوري ( $T_C$ ). وأظهر السلوك الحراري للعينات أنها تتصرف مثل المواد شبه الموصلية. ومن ناحية أخرى، وجد أن هناك تأثير واضح لإضافة أيونات الألومنيوم على التوصيلية الكهربائية ( $\sigma_{DC}$ )، حيث تم تفسير ذلك حسب نظرية القفز الإلكتروني. ومن حساب طاقة التنشيط للعينات تبين أنها تزيد بعد درجة حرارة كوري  $T_C$  عنها قبل هذه الدرجة. وبينت النتائج أن قيم النفاذية المغناطيسية ثابتة عند درجة حرارة الغرفة حتى درجة حرارة كوري  $T_C$  وعندما تصل إلى هذه الدرجة تقل قيمة النفاذية المغناطيسية بسرعة. لقد توافقت قيم الانتقال الحراري  $T_C$  التي تم تحديدها بواسطة نتائج التوصيلية الكهربائية والنفاذية المغناطيسية ووجد أنها تتناقص مع زيادة أيونات الألومنيوم.

